

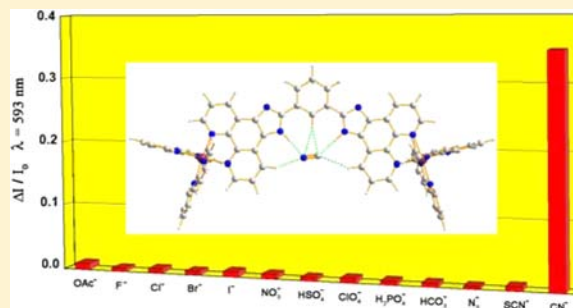
Selective Recognition of Cyanide Anion via Formation of Multipoint NH and Phenyl CH Hydrogen Bonding with Acyclic Ruthenium Bipyridine Imidazole Receptors in Water

Hao-Jun Mo, Yong Shen, and Bao-Hui Ye*

MOE Key Laboratory of Bioinorganic and Synthetic Chemistry, School of Chemistry and Chemical Engineering, Sun Yat-Sen University, Guangzhou 510275, China

Supporting Information

ABSTRACT: Five imidazole-based anion receptors A–E are designed for cyanide anion recognition via hydrogen bonding interaction in water. Only receptors A [Ru(bpy)₂(mpipH)](ClO₄)₂ (bpy is bipyridine and mpipH is 2-(4-methylphenyl)-imidazo[4,5-*f*]-1,10-phenanthroline) and E [Ru₂(bpy)₄(mbpibH₂)](ClO₄)₄ (mbpibH₂ is 1,3-bis([1,10]-phenanthroline-[5,6-*d*]imidazol-2-yl)-benzene) selectively recognize CN[−] from OAc[−], F[−], Cl[−], Br[−], I[−], NO₃[−], HSO₄[−], ClO₄[−], H₂PO₄[−], HCO₃[−], N₃[−], and SCN[−] anions in water (without organic solvent) at physiological conditions via formation of multiple hydrogen bonding interaction with binding constants of $K_{A(H_2O)} = 345 \pm 21$ and $K_{E(H_2O)} = 878 \pm 41$, respectively. The detection limits of A and E toward CN[−] in water are 100 and 5 μM, respectively. Receptor E has an appropriate pK_{a2}^{*} value (8.75) of N–H proton and a C-shape cavity structure with three-point hydrogen bonding, consisting of two NH and one cooperative phenyl CH hydrogen bonds. Appropriate acidity of N–H proton and multipoint hydrogen bonding are both important in enhancing the selectivity and sensitivity toward CN[−] in water. The phenyl CH···CN[−] hydrogen bonding interaction is observed by the HMBC NMR technique for the first time, which provides an efficient approach to directly probe the binding site of the receptor toward CN[−]. Moreover, CN[−] induced emission lifetime change of the receptor has been exploited in water for the first time. The energy-optimized structure of E–CN adduct is also proposed on the basis of theoretical calculations.



INTRODUCTION

Considerable attention has been paid to anion recognition, due to the important roles of anions in various chemical, biological, and environmental processes.^{1–8} Among them, cyanide anion is probably the most toxic one to human body and aquatic life. It inhibits the cellular respiration in mammals by interacting strongly with a heme unit in the active sites of cytochrome *a*₃.⁹ Yet cyanide compounds are still largely used in gold mining and electroplating industries. Accidental discharge of cyanide brings unrecoverable damage to the environment.¹⁰ Optical sensors that can detect cyanide straightforwardly with high sensitivity and selectivity have recently been exploited. However, most of them sense cyanide only in organic solvents or aqueous solvent mixtures, that limits their practical applications. Considerable efforts have been devoted to the development of novel sensors that allow for the recognition and detection of cyanide in genuine aqueous environment.¹¹

Three strategies have been employed to exploit optical sensors for cyanide in recent years.¹² The most popular one is a chemodosimeter approach. In this case, cyanide anion, as a Lewis base or a nucleophile, coordinates to a transition metal center or to an electron-deficient boron, or attacks an electrophilic carbonyl group or a heterocyclic ring system to elicit a detectable change in absorption or emission

spectra.^{13–42} The second one is a coordination complex-based displacement approach, in which the addition of cyanide anion leads to regeneration of spectroscopic behavior.^{43–59} The third strategy combines the binding sites with the signaling subunits via π -conjugated linkers. Interaction of cyanide anion at the binding site via hydrogen bonding causes a detectable change in spectra of the signaling subunit.^{60–71} Such a strategy has been effectively used to detect halide and acetate anions;^{72–76} however, a hydrogen bonded cyanide receptor that operates in pure water has never been reported,¹² though those that sense cyanide in polar solvent^{67,69} or aqueous solvent mixtures^{65,68,70} have been reported. The problems are mainly related to the fact that cyanide anion is highly solvated in water because it has a higher Gibbs energy of hydration ($\Delta G_h^\circ = -295$ kJ/mol),⁷⁷ that depresses the interaction between the receptor and cyanide anion. Moreover, cyanide anion is often involved in protonation equilibria at physiological pH ($pK_a = 9.30$ for HCN in H₂O), so it loses its charge and has less affinity toward weak hydrogen bonding donor. However, cyanide anion is a very strong base in water in contrast to fluoride anion ($pK_a = 3.17$ for HF in H₂O), though their basicities are comparable

Received: January 30, 2012

Published: June 20, 2012

in DMSO ($pK_a = 15$ for HF; $pK_a = 13$ for HCN).⁷⁸ Such differences hint that the pK_a values of the hydrogen bonding donors may play a decisive role in the selective recognition of cyanide anion from the other anions such as fluoride and acetate anions in water.

Recent studies have shown that the receptors with multipoint hydrogen bonding can markedly increase anion affinity, allowing the receptors to tolerate a substantial amount of water from the solvent.^{79–86} On the other hand, Sessler and co-workers have demonstrated that the anion binding affinity of the receptor could be tuned by adjusting the acidity of the N–H proton: stronger acidity leads to stronger anion binding.^{87,88}

These interesting phenomena give us an idea: If a binding site with appropriate N–H acidity is used in water, will its signaling subunit respond to cyanide anion? Following this idea, we utilize ruthenium bpy as a signaling subunit, and imidazo[4,5-*f*]-1,10-phenanthroline as a π -conjugated linker via coordination to Ru(II) center and as a binding site via the NH hydrogen bonding interaction toward cyanide anion. The N–H proton on the imidazole ring becomes appreciably more acidic due to the strong electron-withdrawing effect of Ru(II) ion.^{89–103} Simultaneously, a phenyl ring with various substituents is introduced into the imidazole ring to tune the pK_a value of N–H proton and the phenyl CH hydrogen bonding interaction. In this Article, comparative studies on a series of structural analogues [Ru(bpy)₂(mpipH)](ClO₄)₂ (A), [Ru(bpy)₂(dmpipH)](ClO₄)₂ (B), [Ru(bpy)₂(mopipH)](ClO₄)₂ (C), [Ru(bpy)₂(pmpipH)](ClO₄)₂ (D), and [Ru₂(bpy)₄(mbpibH₂)](ClO₄)₄ (E) (where bpy is 2,2'-bipyridine, mpipH is 2-(4-methylphenyl)-imidazo[4,5-*f*]-1,10-phenanthroline, dmpipH is 2-(2,6-dimethylphenyl)-imidazo[4,5-*f*]-1,10-phenanthroline, mopipH is 2-(4-methoxyphenyl)-imidazo[4,5-*f*][1,10]phenanthroline, pmpipH is 2-(pentamethylphenyl)imidazo[4,5-*f*]-1,10-phenanthroline, and mbpibH₂ is 1,3-bis([1,10]-phenanthroline-[5,6-*d*]imidazol-2-yl)benzene, see Chart 1) provided significant insights into the structural and functional role of pK_a value and phenyl CH cooperative hydrogen bonding in selective recognition of cyanide anion in water. Receptors A and E displayed high selectivity toward cyanide anion without interference from other common anions including fluoride and acetate in water, with significant change in emission spectra and lifetime upon addition of cyanide anion. Particularly, a low detection limit of 5 μ M for receptor E toward cyanide in water is achieved, which is lower than the maximum cyanide contaminant level in drinking water (7.7 μ M) set by the U.S. Environmental Protection Agency.¹⁰⁴

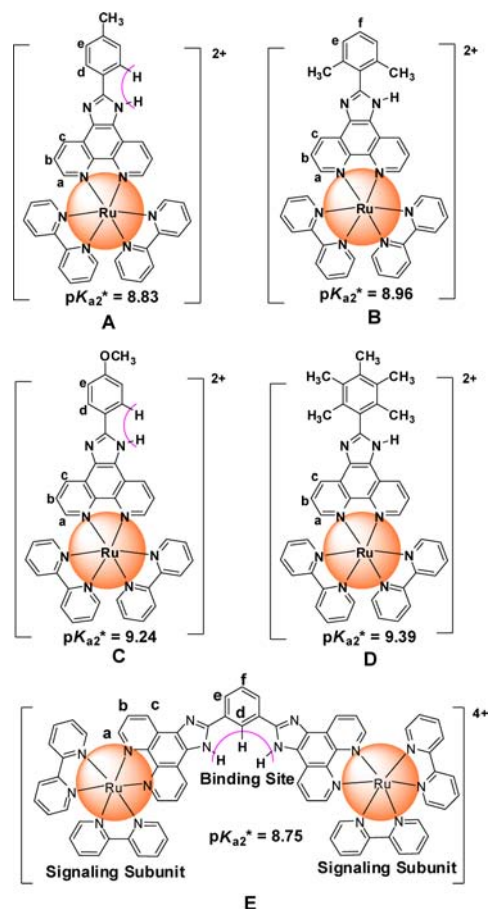
EXPERIMENTAL SECTION

Materials. Reagent grade chemicals obtained from commercial sources were used as received. Deionized water and HPLC DMSO were used in UV and luminescence measurements. DMSO-*d*₆ was used in NMR measurements.

Synthesis. Ru(bpy)₂Cl₂·2H₂O,¹⁰⁵ [Ru(bpy)₂(mpipH)](ClO₄)₂ (A),¹⁰⁶ [Ru(bpy)₂(mopipH)](ClO₄)₂ (C),¹⁰⁶ and [Ru₂(bpy)₄(mbpibH₂)](ClO₄)₄ (E)¹⁰⁷ were synthesized according to literature procedures.

[Ru(bpy)₂(dmpipH)](ClO₄)₂ (B). The ligand dmpipH was synthesized according to literature procedure.^{107–109} The 0.2 mmol Ru(bpy)₂Cl₂·2H₂O, 0.2 mmol dmpipH, and 10 mL ethylene glycol were added to a 50 mL three-neck flask; the mixture was heated at 150 °C and stirred for 12 h under nitrogen protection. Then it was cooled to room temperature and filtered. The filtrate was diluted with 20 mL of distilled water, followed by the addition of excessive NaClO₄. The

Chart 1. Structures of Receptors A–E with Proton Labels



mixture was filtered, and the product was dried in vacuum, yield 78% based on Ru(bpy)₂Cl₂·2H₂O. ¹H NMR (300 MHz, DMSO-*d*₆): δ 9.22 (d, 2H), 8.87 (m, 4H), 8.32 (d, 2H), 8.23 (t, 2H), 8.12 (m, 4H), 7.84 (d, 2H), 7.76 (d, 2H), 7.61 (t, 2H), 7.38 (t, 2H), 7.25 (m, 3H), 2.02 (s, 6H). Anal. Calcd (C₄₁H₃₂N₈Cl₂O₈Ru): C 52.57, H 3.44, N 11.96. Found: C 52.71, H 3.24, N 12.19.

[Ru(bpy)₂(pmpipH)](ClO₄)₂ (D). The ligand pmpipH was synthesized according to literature procedure.^{107–109} The synthetic procedure for D is similar to that of B, yield 82% based on Ru(bpy)₂Cl₂·2H₂O. ¹H NMR (300 MHz, DMSO-*d*₆): δ 8.93 (d, 2H), 8.83 (m, 4H), 8.19 (t, 2H), 8.07 (t, 2H), 8.02 (d, 2H), 7.88 (m, 2H), 7.83 (d, 2H), 7.63 (d, 2H), 7.57 (t, 2H), 7.32 (t, 2H), 2.32 (s, 3H), 2.24 (s, 6H), 1.98 (s, 6H). Anal. Calcd (C₄₄H₃₈N₈Cl₂O₈Ru): C 53.99, H 3.91, N 11.45. Found: C 54.16, H 3.80, N 11.51.

Physical Measurements. Elemental (C, H, and N) analyses were performed on an Elementar Vario EL analyzer. ¹H NMR and ¹H–¹H COSY spectra were obtained on a Varian Mercury-Plus 300 spectrometer, and ¹³C NMR and HMBC spectra were obtained on a Bruker Advance 400 spectrometer. Electronic absorption spectra were obtained on a Shimadzu UV-3150 spectrophotometer. Emission spectra were recorded on a Hitachi F-4500 fluorescence spectrometer. Emission lifetime was obtained on a FLS920 fluorescence lifetime and steady state spectrometer, and a 500 kHz laser beam at 405 nm was used as light source. pH measurements were performed with a Mettler Toledo S20P pH meter equipped with an InLab Science Pro electrode. NMR, UV, and luminescence spectra were recorded at 298 K.

pK_a Determination. A 50 cm³ Robinson–Britton buffer solution consisted of 2.0×10^{-5} M sample was prepared in a 25 °C titration vessel, and magnetic stirring was employed during the whole experiment. A 1 mol dm⁻³ NaOH aqueous solution was added dropwise into the vessel; after each addition, pH value and absorption spectra of the mixed solution were recorded. The pK_a value was fitted from the equation below¹¹⁰

Table 1. Physical Properties of A, B, C, D, E and [Ru(bpy)₃]²⁺ in Water at 298 K

	absorption spectra			emission spectra				
	λ_{\max} (¹ MLCT)/nm	pK _{a1}	pK _{a2}	λ_{\max} (³ MLCT)/nm	Φ	τ /ns	pK _{a1} [*]	pK _{a2} [*]
A	458 ^a	2.26 (±0.07)	9.14 (±0.05)	593 ^a	0.060 ^a	427.16 (±0.45) ^a	2.80 (±0.04)	8.83 (±0.07)
B	459 ^a	2.33 (±0.08)	9.21 (±0.07)	593 ^a	0.058 ^a	423.82 (±0.52) ^a	2.93 (±0.05)	8.96 (±0.06)
C	462 ^a	2.31 (±0.06)	9.53 (±0.06)	596 ^a	0.052 ^a	416.24 (±0.47) ^a	2.85 (±0.05)	9.24 (±0.04)
D	456 ^a	2.45 (±0.05)	9.70 (±0.04)	593 ^a	0.055 ^a	420.80 (±0.39) ^a	2.91 (±0.05)	9.39 (±0.04)
E ^b	461 ^a	1.35 (±0.07)	9.03 (±0.02)	593 ^a	0.073 ^a	441.83 (±0.61) ^a	2.95 (±0.07)	8.75 (±0.05)
[Ru(bpy) ₃] ²⁺	450			593	0.042 ^c	580 ^c		

^aMeasured in 0.02 M HEPES buffer solutions (pH = 7.00). ^bThe determination of pK_{a3} and pK_{a3}^{*} values for E are unsuccessful due to the limited test range of our pH meter (0–12). ^cReference 112.

$$pK_a = \text{pH} - \log \frac{A - A_{\text{HA}}}{A_{\text{A}^-} - A}$$

where A_{HA}, A_{A⁻}, and A refer to the absorbance of the sample at the initial, final, and intermediate pH values at a given wavelength.

pK_a^{*} Determination. The procedure was similar as the one above, except that emission spectra were recorded instead of absorption spectra. The absorbance parameters in the equation were replaced by emission intensity parameters.

Spectroscopic Titration. A 0.05 M HEPES pH = 7.50 or 7.00 water solution consisting of 0.5 or 0.05 M KCN was prepared. Quartz cuvettes with a 1 cm path length and a 3 cm³ volume were used for all measurements. For a typical titration experiment, 10–100 μL aliquots of KCN solution were added to a 2.5 cm³ 0.02 M HEPES pH = 7.50 water solution of A (2.0 × 10⁻⁶ M). (The pH value was adjusted to 7.00 for E, and the concentration of E was 1.0 × 10⁻⁶ M.) For emission titration, the excitation wavelength was 468 nm, the excitation slit width was maintained at 5 mm, and the emission slit width was 10 mm.

Quantum Yield Measurements. Quantum yields were determined in 0.02 M HEPES pH = 7.00 water solution of receptors by a relative method using [Ru(bpy)₃]²⁺ in water as the standard. The quantum yield was calculated by the equation below¹¹¹

$$\Phi_r = \Phi_{\text{std}} \frac{A_{\text{std}} I_r \eta_r^2}{A_r I_{\text{std}} \eta_{\text{std}}^2}$$

where Φ_r and Φ_{std} are the quantum yields of unknown and standard samples ($\Phi_{\text{std}} = 0.042$, 298 K, in water at $\lambda_{\text{ex}} = 450$ nm),¹¹² A_r and A_{std} are the solution absorbance at the excitation wavelength (λ_{ex}), I_r and I_{std} are the integrated emission intensities, and η_r and η_{std} are the reflective indices of the solvent. Experimental error in the reported luminescence quantum yield was about 20%.

Theoretical Calculations. Theoretical calculations were performed on E–CN adduct to optimize the structure and calculate the ¹³C NMR chemical shift of CN⁻ with density functional theory (DFT), using the Gaussian 03 program package¹¹³ with the B3LYP method^{114–116} and the 6-31G* basis set¹¹⁷ for hydrogen, carbon, and nitrogen atoms and the Stuttgart/Dresden (SDD) energy-consistent pseudopotentials for ruthenium.^{118,119}

RESULTS AND DISCUSSION

Syntheses and Characterization of the Receptors. The ligands were synthesized on the basis of the approach established by Steck et al.¹²⁰ and developed by our group.^{107–109} Condensation of 1,10-phenanthroline-5,6-dione with substituent benzaldehyde or isophthalic aldehyde in refluxing glacial acetic acid in the presence of ammonium acetate afforded the corresponding ligand. Introduction of substituents to the phenyl ring at various sites could yield various functions. The electron-donating groups, such as methyl and methoxyl, can indeed enhance the pK_a value of imidazole N–H proton and tune its anion binding capability.^{87,121} Furthermore, the substituents at various

positions would affect the binding modes of receptors toward anions, in particular, multipoint hydrogen bonding interaction and function of phenyl CH cooperative hydrogen bonding. The complexes A–E were obtained by the reaction of Ru(bpy)₂Cl₂ with the corresponding ligands in ethylene glycol. All these complexes were characterized by elemental analyses and NMR spectra.

The absorption and emission bands are 458 and 593 nm for A, 459 and 593 nm for B, 462 and 596 nm for C, 456 and 593 nm for D, and 461 and 593 nm for E in HEPES buffer solution. They are pH dependent because of the protonation or deprotonation of the imidazole ring. Variation of the pH value affects the protonation state of imidazole nitrogen atoms, and the π* energy levels of the imidazole phenanthroline ligands are changed accordingly.¹²² The various deprotonation steps for A, and B, C, D, and E are shown in Schemes S1 and S2 in the Supporting Information, respectively. Their ground state pK_a values are determined by absorption spectra (see Figures S1–S3), and the excited state pK_a^{*} values are determined by emission spectra (see Figures S4–S8). As shown in Table 1, the excited state pK_{a1}^{*} values of A, B, C, D, and E are 2.80 ± 0.04, 2.93 ± 0.05, 2.85 ± 0.05, 2.91 ± 0.05, and 2.95 ± 0.07, respectively, which are all greater than the respective ground state pK_{a1} values (2.26 ± 0.07 for A, 2.33 ± 0.08 for B, 2.31 ± 0.06 for C, 2.45 ± 0.05 for D, and 1.35 ± 0.07 for E). The emission spectra of these complexes all undergo about 15 nm blue-shift with a concomitance of intensity enhancement as the solutions change from acidic to neutral. These phenomena give us an insight into the MLCT nature of complexes A–E. In acidic solution, all nitrogen atoms of imidazole ring are protonated, the π* energy level of imidazo[4,5-f]-1,10-phenanthroline ligand is a little lower than that of bpy ligand, and the excited electron goes to imidazo[4,5-f]-1,10-phenanthroline ligand from Ru center. This makes the N–H fragment of imidazole ring more basic in the excited state, so the pK_{a1}^{*} value is greater than the ground state pK_{a1} value. When the solution becomes neutral, one of the nitrogen atoms of imidazole ring is deprotonated. The π* energy level of imidazo[4,5-f]-1,10-phenanthroline ligand rises, inducing a change in the MLCT nature, where the excited electron goes to bpy ligand from Ru center, resulting in a significant blue shift in the emission spectra with a concomitant emission intensity enhancement. However, emission intensity is reduced by 37%, 36%, 37%, 38%, and 48% for A, B, C, D, and E, respectively, upon increasing the pH value from 7 to 10 (see Figures S4–S8), with a minor 4–7 nm red-shift in the emission maximum. Further increase of the pH value does not induce any more spectral change because the two nitrogen atoms on the imidazole ring are deprotonated. The pK_{a2}^{*} values of 8.83 ± 0.07 for A, 8.96 ± 0.06 for B, 9.24 ± 0.04 for C, 9.39 ± 0.04 for

D, and 8.75 ± 0.05 for E are lower than the respective ground state pK_{a2} values (9.14 ± 0.05 for A, 9.21 ± 0.07 for B, 9.53 ± 0.06 for C, 9.70 ± 0.04 for D, and 9.03 ± 0.02 for E), indicating that the excited electron is located on bpy ligand, which renders the ruthenium center and the N–H proton of imidazole ring more acidic in the excited state.¹²³

From the profiles of intensity variety against various pH values, we can find that the stable absorption and emission pH ranges in water are 3.70–7.80 and 4.50–7.50 for A, 3.90–7.95 and 4.45–7.70 for B, 3.85–8.40 and 4.50–7.90 for C, 3.60–8.80 and 4.40–8.00 for D, and 2.90–7.60 and 5.10–7.00 for E. In these pH regions, the ligands are neutral, and complexes are strong emitters. In pH = 7.00 0.02 M HEPES solutions at 298 K, the quantum yields and the lifetimes of the ³MLCT excited states are 0.060 and 427.16 ± 0.45 ns for A, 0.058 and 423.82 ± 0.52 ns for B, 0.052 and 416.24 ± 0.47 ns for C, 0.055 and 420.80 ± 0.39 ns for D, and 0.073 and 441.83 ± 0.61 ns for E. These values are comparable to those of the noted complex $[\text{Ru}(\text{bpy})_3]^{2+}$ ($\Phi = 0.042$ and $\tau = 580$ ns).¹¹² The strong emitting nature of these complexes allows us to employ them at a micromolar concentration level in anion sensing studies.

Selective Recognition of Receptor A toward Cyanide Anion in Water. Anion recognition study of A was first carried out with an emission spectral experiment in a HEPES buffer solution at pH = 7.50, as the emission intensity was about to drop after this pH point (Figure S4). As shown in Figure 1, A

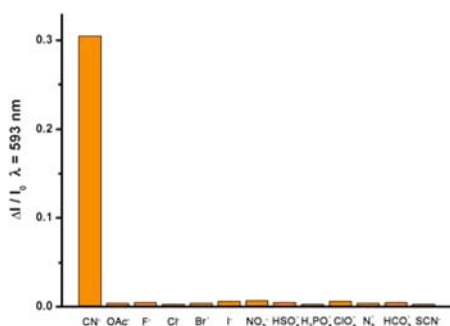


Figure 1. Relative emission response of A ($2.0 \mu\text{M}$ in pH = 7.50 0.02 M HEPES buffer) at 593 nm in the presence of 8 mM K^+ salts of CN^- , OAc^- , F^- , Cl^- , Br^- , I^- , NO_3^- , HSO_4^- , H_2PO_4^- , ClO_4^- , N_3^- , HCO_3^- , and SCN^- .

exhibited no response to OAc^- , F^- , Cl^- , Br^- , I^- , NO_3^- , HSO_4^- , ClO_4^- , H_2PO_4^- , HCO_3^- , N_3^- , and SCN^- anions, except for CN^- with decreased emission intensity in water. Its response ability toward CN^- was unaffected by the presence of all other anions (see Figure S9), indicating high selectivity of A toward CN^- in water.

Emission titration experiment of A with CN^- was also carried out. As shown in Figure 2, the emission spectra of A underwent gradual decrease upon addition of CN^- , the intensity was decreased by 31%, and the emission peak had a 6 nm minor red-shift when the concentration of CN^- reached 8 mM. No more change was observed upon further addition of CN^- . Job plot analysis indicated a 1:1 A–CN adduct in water (Figure S10). The titration curve is hyperbolic; a 1:1 binding equation is used to calculate the binding constant¹²⁴

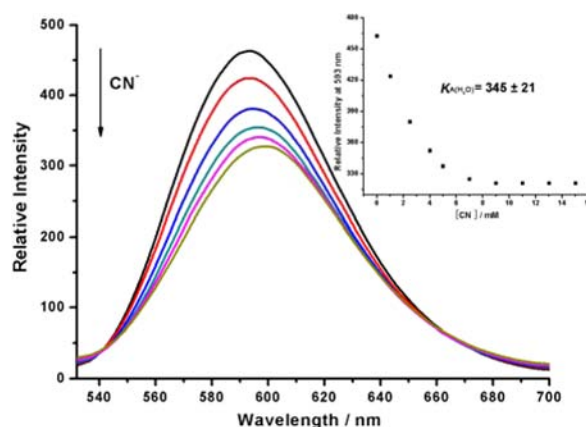


Figure 2. Emission spectral titration of A ($2.0 \mu\text{M}$ in pH = 7.50 0.02 M HEPES buffer) with CN^- ($\lambda_{\text{ex}} = 468$ nm). Inset: Emission intensity at 593 nm versus concentration of CN^- , with binding constant calculated from a 1:1 binding model.

$$\Delta I = \left(\Delta \epsilon \left([H] + [G] + \frac{1}{K} \right) \pm \sqrt{\Delta \epsilon^2 \left([H] + [G] + \frac{1}{K} \right)^2 - 4 \Delta \epsilon^2 [H][G]^{1/2}} \right) \quad (1)$$

where $[H]$ and $[G]$ are the concentrations of A and CN^- , ΔI is the change of emission intensity at 593 nm, $\Delta \epsilon$ is the change of molar emission intensity, and K is the binding constant. A binding constant $K_{A(\text{H}_2\text{O})} = 345 \pm 21$ is achieved. The Stern–Volmer plot for this titration process is shown in Figure S11, giving a Stern–Volmer constant $K_{\text{SV}} = 0.069 \pm 0.004 \text{ M}^{-1}$ for bimolecular excited state quenching.¹²⁵ Division of this K_{SV} value by the lifetime of photoexcited A ($\tau_0 = 427.16$ ns in water) yields a bimolecular quenching rate constant $k_q = 1.61 \times 10^5 \text{ M}^{-1} \text{ s}^{-1}$. The detection limit of A toward CN^- is $100 \mu\text{M}$ by the $\text{S/N} > 3$ approach (Figure S12). The absorption spectra of A in water only had a 4 nm red-shift on the MLCT band upon addition of a large excess of CN^- (Figure S13).

For comparison purpose, emission titration experiment of A with CN^- was also performed in DMSO solution (Figure S14). A 5 nm red-shift of the emission peak was observed upon addition of 1 equiv of CN^- ; the emission intensity was reduced by 34%. Further addition of CN^- caused no more change. These changes are comparable to those observed in H_2O . However, attempt to get the binding constant by nonlinear fitting was unsuccessful, because the curvature in the titration profile was too steep to allow a safe determination.¹²⁶

It is obvious that the affinity of A toward CN^- is much weaker in water than in DMSO. The much higher solvation energy of CN^- in water ($\Delta G_{\text{h}}^\circ = -295 \text{ kJ/mol}$)⁷⁷ may account for this phenomenon. However, A had no interaction with other anions that have a comparable hydration energy ($\Delta G_{\text{h}}^\circ$ to cyanide anion (-365 , -340 , -315 , -300 , and -295 kJ/mol for OAc^- , Cl^- , Br^- , NO_3^- , and N_3^- , respectively)).⁷⁷ Here comes a question: Why does A only respond to CN^- in water? The much stronger basicity of CN^- in water may be the main reason. The pK_{a} value of HCN in water (9.30) is much higher than that of other acid ($pK_{\text{a}} = 4.75$ for HOAc and 4.72 for HN_3 in water).

When the strong basic CN^- anion gets close to the acidic N–H fragment of A, hydrogen bonding interaction occurs, which leads to a partial proton transfer from the ligand to CN^-

and an increase of electron density on Ru center, resulting in the minor red-shifts of the absorption and emission spectra and decrease of emission intensity.¹²⁷

To further understand the nature of hydrogen bonding interaction of **A** toward CN^- , NMR experiments were performed for **A** in the absence and presence of CN^- in $\text{DMSO}-d_6$. NMR spectral change for **A** upon addition of CN^- stopped at 1 equiv of the anion, and further addition of CN^- induced no more change. As shown in Figure 3, addition of

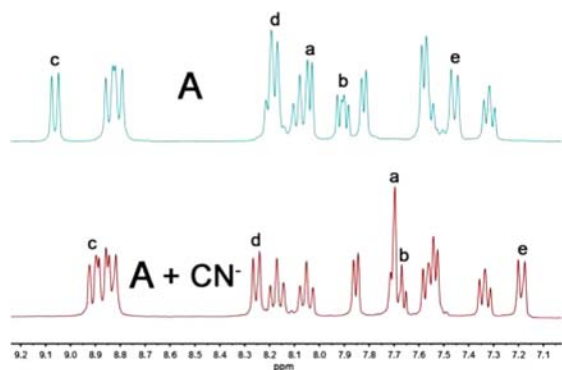


Figure 3. ^1H NMR spectra of **A** (0.01 M) in $\text{DMSO}-d_6$ in the absence and presence of 1 equiv of CN^- (298 K, 300 MHz).

CN^- into **A** caused 0.2–0.4 ppm upfield shifts for proton signals of a, b, c, and e (the assignments of these signals are based on $^1\text{H}-^1\text{H}$ COSY spectrum, see Figures S15 and S16), due to hydrogen bonding interaction between CN^- and N–H fragment of imidazole ring, which led to a partial proton transfer from the ligand to CN^- and electron density increase on the ligand. In contrast, the proton d signal of **A** displayed an observable downfield shift of 0.08 ppm, which gave us an idea that direct hydrogen bonding between proton d and CN^- might occur. To prove this supposition, the HMBC (heteronuclear multiple bond coherence) NMR experiment was performed. As shown in Figure 4, a clear correlation point between the proton d signal and the cyanide carbon signal was observed. Therefore, a two-point hydrogen bonding model between **A** and CN^- is established, in which the NH and CH hydrogen bonding donors cooperatively participate in cyanide anion binding. To the best of our knowledge, this affords the

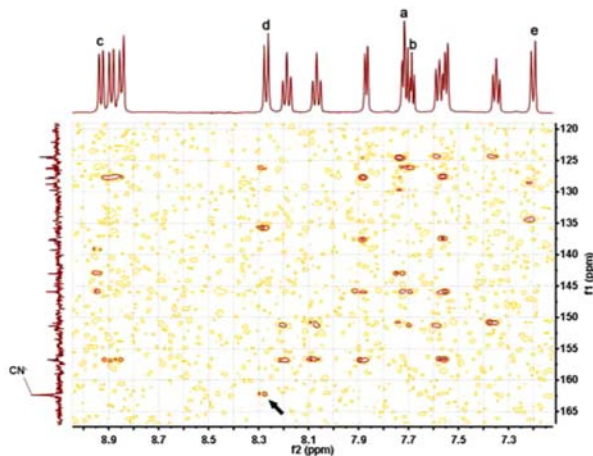


Figure 4. HMBC spectrum of **A** (0.01 M) in $\text{DMSO}-d_6$ in the presence of 1 equiv of CN^- (298 K, 400 MHz).

direct evidence for hydrogen bonding interaction between the proton of phenyl CH and carbon of CN^- via HMBC NMR technique for the first time.^{12–14} The finding here provides an effective approach to directly observe the binding site of the receptor toward CN^- and helps to understand the mechanism of CN^- sensor. It is a very rare phenomenon for a neutral phenyl C–H proton to directly engage in hydrogen bonding toward an anion.^{71,128} The instance of hydrogen bonding interaction between the imidazolium CH and CN^- has also been observed by X-ray single crystal diffraction.¹²⁹

Insight into the Function of Phenyl C–H Cooperative Hydrogen Bonding toward Cyanide Anion.

The fact that two-point hydrogen bonding of **A** played an important role for selective recognition of CN^- in water prompted us to examine the function of phenyl CH hydrogen bonding interaction toward CN^- . Receptor **B** with a comparable $\text{p}K_{a2}^*$ value (8.96 in H_2O) to that of **A** (8.83) but without phenyl CH cooperative hydrogen bonding was synthesized. No spectral response was observed for **B** upon addition of CN^- in H_2O under the experiment conditions (pH = 7.70 0.02 M HEPES solution). However, emission spectral titration of **B** in DMSO showed a 4 nm red-shift of the emission peak with 32% decrease of intensity upon addition of 2 equiv of CN^- . A binding constant of $K_{B(\text{DMSO})} = (2.15 \pm 0.15) \times 10^6$ was calculated by fitting of eq 1 (see Figures S17 and S18). ^1H NMR spectra in $\text{DMSO}-d_6$ showed 0.23–0.38 ppm upfield shifts for proton signals of a, b, c, e, and f upon addition of 1 equiv of CN^- (see Figures 5 and

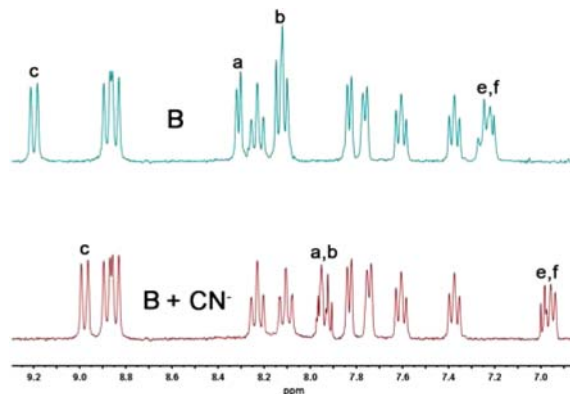


Figure 5. ^1H NMR spectra of **B** (0.01 M) in $\text{DMSO}-d_6$ in the absence and presence of 1 equiv of CN^- (298 K, 300 MHz).

S19), which was a typical phenomenon when hydrogen bonding occurred. The fact that there is no spectral response of **B** toward CN^- in H_2O and weaker interaction of **B** toward CN^- in DMSO indicates that the importance of incorporating phenyl CH hydrogen bonding is obvious in recognition of CN^- in water. The strong binding affinity of **A** toward CN^- should benefit from the synergetic effect of the dual hydrogen bonding interactions. The cooperative NH and phenyl CH hydrogen bonding interaction is capable of capturing CN^- in H_2O . The observations here indicate that the multipoint, synergetic hydrogen bonding interaction, including N–H \cdots CN^- hydrogen bonds and the weaker phenyl C–H \cdots CN^- hydrogen bond, plays an important role in selective recognition of CN^- in water.

Insight into the Influence of N–H $\text{p}K_{a2}^*$ Value on Binding Affinity toward Cyanide Anion. Recent studies have demonstrated that the N–H $\text{p}K_{a2}^*$ value of receptor would tune the binding affinity toward anion.^{87,88} Following this idea,

the stronger electron-donating substituent methoxyl was used to displace the methyl group in **A** to increase the N–H pK_{a2}^* value, where the potential phenyl CH hydrogen bonding still exists (see Chart 1). Indeed, the pK_{a2}^* value of **C** is 9.24 in water, higher than that of **A** (8.83). To observe the interaction of **C** toward CN^- , emission experiments of receptor **C** were performed in the absence and presence of CN^- in water. However, no detectable spectral change was observed for **C** upon addition of CN^- in water. 1H NMR spectra in $DMSO-d_6$ showed 0.16–0.34 ppm upfield shifts for proton signals of a, b, c, and e upon addition of 1 equiv of CN^- (Figures S20–S22). The proton d signal displayed a 0.06 ppm downfield shift, due to phenyl CH hydrogen bonding with CN^- . The HMBC experiment also showed a clear correlation point between CN^- carbon signal and the proton d signal, verifying the phenyl CH hydrogen bonding interaction with CN^- carbon (Figure S23). Moreover, emission spectral titration of **C** upon addition of CN^- was carried out in DMSO. A 4 nm red-shift of the emission band and a 34% intensity decrease were observed upon addition of 2 equiv of CN^- (Figure S24). Job plot analysis showed a 1:1 stoichiometry for **C**– CN^- interaction in DMSO (Figure S25). The binding constant of **C** toward CN^- is $K_{C(DMSO)} = (6.54 \pm 0.41) \times 10^6$, which is much weaker than that of **A** (the binding constant K_A in DMSO is too large to measure, estimated to be greater than 10^7). This may explain why no spectral change of **C** was observed upon addition of CN^- in water. The weaker binding affinity between **C** and CN^- cannot prevent CN^- from hydration when water is used as solvent, because CN^- has a high Gibbs energy of hydration,⁷⁷ that depresses the interaction of **C** toward CN^- in water. The observations here indicate that the selective recognition of CN^- in water can be achieved by tuning the pK_a value of hydrogen bonding donating segment.

To further compare the binding affinity, receptor **D** with higher pK_{a2}^* value (9.39) than that of **B** (8.96) and without phenyl CH hydrogen bonding was introduced (see Chart 1) and its interaction toward CN^- was also observed in DMSO. The titration profile of **D** was a smooth hyperbolic curve (Figure S26). The 1:1 **D**– CN^- stoichiometry was proved by Job plot analysis (see Figure S27). A binding constant $K_{D(DMSO)} = (1.16 \pm 0.07) \times 10^6$ is obtained by well fitting eq 1, which is half the value of **B** ($K_{B(DMSO)} = 2.15 \times 10^6$). When the pK_{a2}^* value rises from 8.96 (**B**) to 9.39 (**D**), the acidity of NH proton is decreased. This difference in acidity makes the hydrogen bonding affinity of **D** toward CN^- weaker than that of **B** in DMSO.

Highly Selective and Sensitive Receptor E toward Cyanide Anion in Water. The aforementioned studies demonstrated that the pK_{a2}^* value of the imidazolyl NH played a crucial role in the selective recognition of CN^- from the other anions in water: the stronger acidity led to the stronger CN^- binding affinity. Simultaneously, this recognition process is cooperated with the formation of phenyl CH hydrogen bonding. The multipoint hydrogen bonding interaction incorporating NH and CH donor groups greatly enhances the sensitivity of receptor toward anion. With these in mind, a binuclear ruthenium complex **E** is used to recognize CN^- in water. The bridge ligand mbpibH₂ connects two signaling Ru(bpy)₂ segments with a planar structure, resulting in a C-shape acyclic cavity (see Chart 1) with multiple hydrogen bonding interactions toward CN^- .^{130,131} In the meantime, the NH protons on the imidazole rings become appreciably more acidic due to the dual strong electron-

withdrawing effect of Ru(II) ions. Indeed, the pK_{a2}^* value of **E** is 8.75 in water, that is lower than those of **A** (8.83), **B** (8.96), and **C** (9.24). These will indeed augment the binding affinity of **E** toward CN^- . Moreover, the binding affinity would profit from the acidity increase of the bridging phenyl proton because of the two substituents of electron-withdrawing imidazolyl groups.

To examine our hypothesis, an emission titration experiment of **E** with CN^- was carried out in the HEPES buffer solution at pH = 7.00. The emission spectra of **E** underwent gradual decrease upon addition of CN^- . The intensity was maximally decreased by 34% with a concomitant 5 nm red-shift of emission peak when the concentration of CN^- reached 6 mM (see Figure 6). No more change was observed upon further

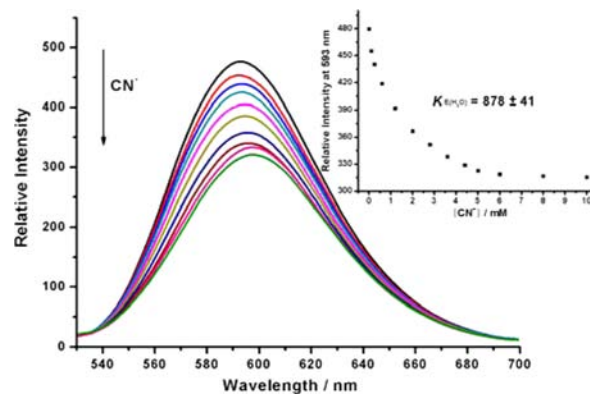


Figure 6. Emission spectral titration of **E** (1.0 μ M in pH = 7.00 0.02 M HEPES buffer) with KCN. Inset: Emission intensity at 593 nm versus concentration of CN^- , with binding constant calculated from a 1:1 binding model.

addition of CN^- . Job plot approach was applied to analyze the stoichiometry of the **E**– CN^- adduct, indicating a 1:1 stoichiometry adduct formation in water (Figure S28). A binding constant of **E** toward CN^- in water $K_{E(H_2O)} = 878 \pm 41$ was calculated from eq 1. This is 2.5 times larger than that of **A** ($K_{A(H_2O)} = 345$). The Stern–Volmer plot for this titration process is shown in Figure S29, giving a Stern–Volmer constant $K_{SV} = 0.100 \pm 0.005 M^{-1}$ and a bimolecular quenching rate constant $k_q = 2.26 \times 10^5 M^{-1} s^{-1}$. These are larger than the values of **A** ($K_{SV} = 0.069 M^{-1}$ and $k_q = 1.61 \times 10^5 M^{-1} s^{-1}$), indicating that **E** is a stronger proton donor than **A**. The detection limit of **E** toward CN^- was determined to be 5 μ M by the $S/N > 3$ approach (Figure S30). This is 20 times lower than that of **A** (100 μ M) and lower than the maximum cyanide contaminant level in drinking water (7.7 μ M) set by the U.S. Environmental Protection Agency.¹⁰⁴ The absorption spectra of **E** in water only had a 5 nm red-shift on the MLCT band upon addition of a large excess of CN^- (Figure S31).

To examine the selectivity of receptor **E** toward anions, the influences of other anions such as OAc^- , F^- , Cl^- , Br^- , I^- , NO_3^- , HSO_4^- , ClO_4^- , $H_2PO_4^-$, HCO_3^- , N_3^- , and SCN^- on the emission spectra of **E** in a HEPES buffer solution were observed. The addition of the aforementioned anions to the solution of **E** resulted in negligible spectral change under the identical conditions of CN^- , as shown in Figure 7, indicating that receptor **E** is highly selective toward CN^- among the observed anions in water. Moreover, the antidisturbance experiments of receptor **E** were also conducted. Its response ability toward CN^- was unaffected by the presence of the

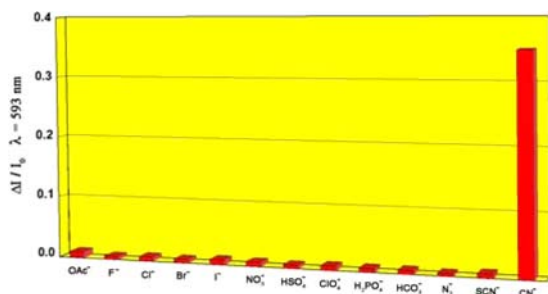


Figure 7. Relative emission response of E ($1.0 \mu\text{M}$ in $\text{pH} = 7.00$ 0.02 M HEPES buffer) at 593 nm in the presence of 5 mM K^+ salts of OAc^- , F^- , Cl^- , Br^- , I^- , NO_3^- , HSO_4^- , ClO_4^- , H_2PO_4^- , HCO_3^- , N_3^- , SCN^- , and CN^- .

and OAc^- . However, the proton d signal displayed an obvious downfield shift from 9.33 to 9.48 ppm , because of direct hydrogen bonding between proton d and CN^- . HMBC spectra showed a clear correlation point between the proton d signal and the cyanide carbon signal, verifying the phenyl C–H hydrogen bonding interaction toward CN^- carbon atom (Figure 10). This hydrogen bonded interaction is much weaker than those observed in $\text{N-H}\cdots\text{CN}^-$, because of the weak acidity of the C–H proton.

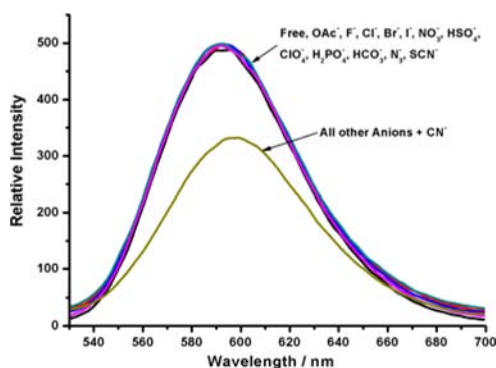


Figure 8. Emission spectra of E ($1.0 \mu\text{M}$ in $\text{pH} = 7.00$ 0.02 M HEPES buffer) in the presence of 5 mM K^+ salts of OAc^- , F^- , Cl^- , Br^- , I^- , NO_3^- , HSO_4^- , ClO_4^- , H_2PO_4^- , HCO_3^- , N_3^- , and SCN^- , respectively, and in the presence of 5 mM KCN plus the aforementioned anions.

Moreover, an emission titration experiment of E with CN^- was also performed in DMSO solution (Figure S32). Similar phenomena were found such that, in water, a 3 nm red-shift of the emission peak and 35% emission intensity decrease were observed upon addition of 1 equiv of CN^- . However, the binding constant was too large to be calculated by nonlinear fitting, because the curvature in the titration profile was too steep to allow a safe determination.¹²⁶

To further understand the mechanism of receptor E toward CN^- , NMR experiments were performed in the absence and presence of CN^- in $\text{DMSO-}d_6$. NMR spectral change for E stopped at the addition of 1 equiv of CN^- ; further addition of CN^- induced no more change. As shown in Figures 9 and S33, addition of CN^- into E caused 0.20 – 0.36 ppm upfield shifts for the a, b, c, e, and f proton signals and disappearance of the N–H signal, due to strong hydrogen bonding between CN^- and N–H fragments of the imidazole ring. It is well-known that the imidazole N–H protons in E are more acidic and form strong hydrogen bonds with CN^- , which led to a partial proton transfer from the ligand to CN^- and electron density increase on the ligand; finally, the N–H signal disappears and non-hydrogen-bonded C–H protons shift to upfield. This is a normal phenomenon when strong hydrogen bonding interaction occurs and was also reported by Morales' group¹³² and Baitalik's group,⁹⁹ in which the signals of N–H protons disappeared upon hydrogen bonding with anions such as Cl^-

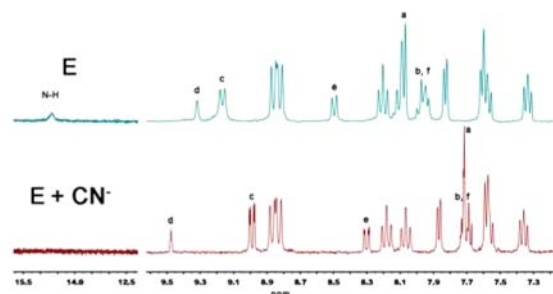


Figure 9. ^1H NMR spectra of E (0.01 M) in $\text{DMSO-}d_6$ in the absence and presence of 1 equiv of CN^- (298 K , 300 MHz).

and OAc^- . However, the proton d signal displayed an obvious downfield shift from 9.33 to 9.48 ppm , because of direct hydrogen bonding between proton d and CN^- . HMBC spectra showed a clear correlation point between the proton d signal and the cyanide carbon signal, verifying the phenyl C–H hydrogen bonding interaction toward CN^- carbon atom (Figure 10). This hydrogen bonded interaction is much weaker than those observed in $\text{N-H}\cdots\text{CN}^-$, because of the weak acidity of the C–H proton.

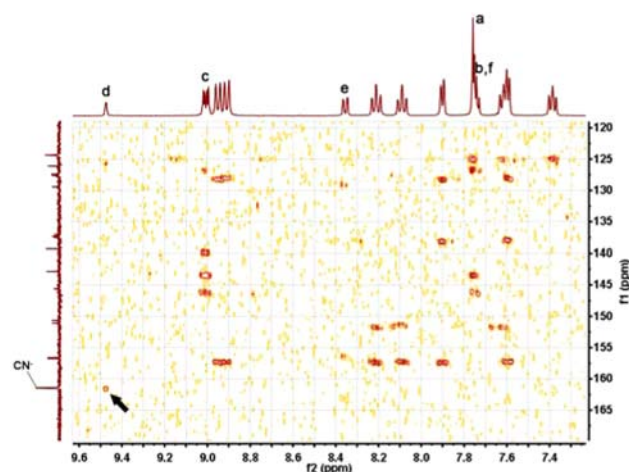


Figure 10. HMBC spectrum of E (0.01 M) in $\text{DMSO-}d_6$ in the presence of 1 equiv of CN^- (298K , 400 MHz).

Upon combination of Job plot analysis in $1:1 \text{ E-CN}$ adduct and NMR experiments, therefore, a three-point hydrogen bonding interaction model between receptor E and CN^- is proposed, in which cyanide anion is anchored at the C-shape cavity (see Chart 1) and further stabilized by the formation of two imidazole $\text{N-H}\cdots\text{CN}^-$ hydrogen bonds and one phenyl $\text{C-H}\cdots\text{CN}^-$ hydrogen bond. The excellent selectivity of E toward CN^- can be attributed to the fitness in the acidity of its NH groups in imidazole rings, which is tuned to be able to distinguish the subtle difference in the affinity of CN^- to proton in water.

Relationship between the Binding Affinity and ^{13}C NMR Chemical Shift of Cyanide Anion. The binding affinity of receptors A–E toward CN^- is much dependent on the $\text{p}K_{\text{a}2}^*$ value of NH proton and the multipoint hydrogen bonding. The stronger acidity leads to stronger binding affinity because of its stronger proton donor capability. During this course, a partial proton of NH segment transfers to CN^- carbon via hydrogen bonding,¹³³ leading to change of electron density on CN^- carbon atom. Such subtle change may be directly reflected by

^{13}C chemical shift of CN^- carbon. Therefore, systematic observations of the ^{13}C NMR spectra may provide sufficient information for the binding affinity. This is the indeed case. The ^{13}C chemical shift of free CN^- in $\text{DMSO}-d_6$ is 166.44 ppm, which undergoes different extent of upfield shifts to 162.39, 162.91, 162.68, 163.16, and 161.85 ppm in the presence of receptors of A, B, C, D, and E, respectively (see Figure 11), due

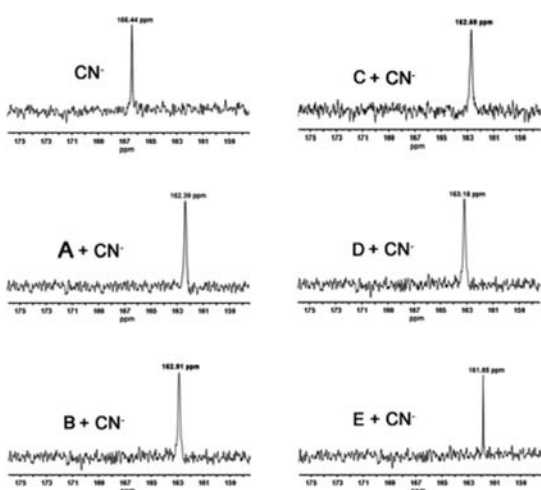


Figure 11. ^{13}C NMR spectra of CN^- (0.01 M) in $\text{DMSO}-d_6$ in the absence and presence of 1 equiv of receptors A–E.

to the formation of hydrogen bonding. This upshift trend is consistent with the binding affinity between the receptors and CN^- in DMSO ($K_B = 2.15 \times 10^6$, $K_C = 6.54 \times 10^6$, and $K_D = 1.16 \times 10^6$): the stronger binding affinity via hydrogen bonding interaction leads to a larger upfield shift of the CN^- carbon signal. The observations here indicate that ^{13}C NMR spectrum is an efficient technique to monitor the interaction strength between the receptor and CN^- via hydrogen bonding.

Detection of Cyanide Anion via Time-Resolved Emission in Water. Receptors A and E are strong emitters in water. Their extraordinary feature allows us to perform time-resolved emission study on A and E in water upon addition of CN^- . The free receptors and their CN^- adducts may have different emission lifetimes, because a robust hydrogen bonding interaction in the latter species leads to a partial proton transfer from N–H fragment to CN^- , resulting in a decrease of its emission lifetime. Time-resolved emission provides information on the excited state kinetics and heterogeneity of different emissive species in a system.^{134,135} Figures 12 and S34 present the emission lifetime quenching of receptors A and E as a function of CN^- concentration. Lifetimes and component fraction were calculated by nF900 software package. They displayed single-exponential decay with lifetimes of 427.05 ± 0.41 ns for A and 441.83 ± 0.61 ns for E in the absence of CN^- . Upon addition of CN^- , the emission decays became biexponential. The new short-lived components with lifetimes of 278.24 ± 5.35 ns for A and 266.83 ± 6.32 ns for E appeared, and their fractions increased as the CN^- concentration increased. When the concentrations of CN^- reached 7 mM for A and 5 mM for E, the fraction of short-lived components rose to 74.8% for A and 79.1% for E. Further addition of CN^- induced no more change. To the best of our knowledge, such emission lifetime anion titration has never been conducted in water,³⁹ due to complete quenching of most emissive compounds by water.

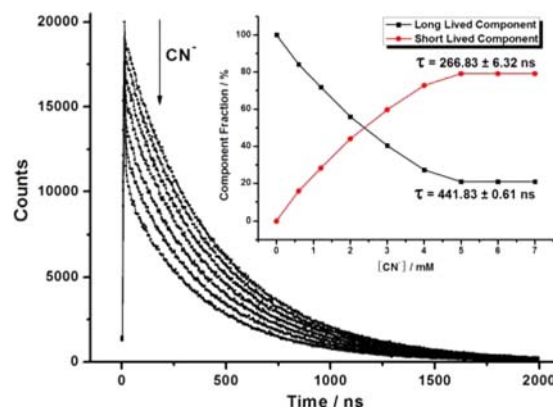


Figure 12. Emission decay profiles of E ($1.0 \mu\text{M}$ in $\text{pH} = 7.00$ 0.02 M HEPES buffer) upon addition of KCN ($\lambda_{\text{ex}} = 405 \text{ nm}$, $\lambda_{\text{em}} = 593 \text{ nm}$). Inset: Change of fractions of the two lifetime components as the concentration of CN^- increased.

Theoretical Analysis and Interaction Model of Receptor E and Cyanide Anion. Theoretical calculations were performed on E– CN^- adduct to optimize the structure and calculate the ^{13}C NMR chemical shift of CN^- , using the Gaussian 03 program package¹¹³ with the B3LYP method^{114–116} and the 6-31G* basis set¹¹⁷ for hydrogen, carbon, and nitrogen atoms and the Stuttgart/Dresden (SDD) energy-consistent pseudopotentials for ruthenium.^{118,119} As expected, CN^- is anchored at the C-shape cavity, in which receptor E donates five-point hydrogen bond to CN^- in the energy-minimized structure (see Figure 13). The bond length of CN^-

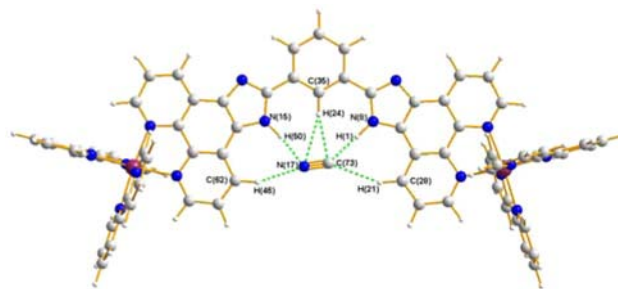


Figure 13. Optimized structure of E– CN^- using the B3LYP method and the 6-31G* basis set for hydrogen, carbon, and nitrogen atoms and the SDD energy-consistent pseudopotentials for ruthenium. The selected distances (Å) and angles (deg): C(73)–N(17), 1.18; N(8)···C(73), 2.91; N(15)···N(17), 2.86; C(35)···C(73), 3.41; C(35)···N(17), 3.61; C(28)···C(73), 3.64; C(62)···N(17), 3.38; N(8)–H(1)–C(73), 179.04; N(15)–H(50)–N(17), 172.12; C(35)–H(24)–C(73), 168.52; C(35)–H(24)–N(17), 164.16; C(28)–H(21)–C(73), 155.55; C(62)–H(46)–N(17), 156.99.

is 1.18 Å, comparable to that observed in crystal structure of 1,3-diisopropyl-4,5-dimethylimidazolium cyanide (1.120(7) Å).¹²⁹ The two imidazole NH protons are indeed hydrogen bonded to CN^- with distances of N(8)···C(73) 2.91 Å and N(15)···N(17) 2.86 Å. The CH proton H24 (d) of the bridged phenyl ring is hydrogen bonded to CN^- with distances of C(35)···C(73) 3.41 Å and C(35)···N(17) 3.61 Å, which is in agreement with the HBMC experiment. The optimized model of CN^- is consistent with that observed in crystal structure of 1-isopropyl-3,4,5-trimethylimidazolium cyanide, in which the imidazolium proton is hydrogen bonded to CN^- with distances of C···C 3.428 Å and C···N 3.372 Å.¹²⁹ The H46 and H21 (c)

are also hydrogen bonded to CN⁻ with distances of C(28)–C(73) 3.64 Å and C(62)–N(17) 3.38 Å. However, no correlation signal was observed in the HMBC experiment, maybe due to the longer distance between them. When DMSO is employed as solvent and TMS (tetramethylsilane, Si(CH₃)₄) as a reference, the calculated carbon CN⁻ chemical shift of free cyanide is 170.50, and that of E–CN adduct is 167.37 ppm, indicating a 3.13 ppm upfield shift. This is close to the 4.59 ppm upfield shift observed from experiment.

CONCLUSIONS

In conclusion, two cyanide receptors A and E with high selectivity in water via hydrogen bonding interaction have been exploited at physiological conditions. Receptor E possesses an appropriate pK_{a2}^{*} value of N–H proton and a C-shape cavity structure with three-point hydrogen bonding donating to CN⁻, consisting of N–H and phenyl C–H hydrogen bonds, with a detection limit as low as 5 μM in water. The multipoint hydrogen bonding includes the weak cooperative phenyl C–H hydrogen bonding and an appropriate acidity of N–H proton, which are both important in enhancing the selectivity and sensitivity of receptor toward CN⁻ in water. Moreover, we have exploited the first sensor based on the direct observation of CN⁻ induced emission lifetime changes in water and applied the HMBC technique to directly investigate the binding site of the receptor toward CN⁻ via hydrogen bonding. These help to understand the mechanism of the CN⁻ sensor and provide a new strategy to develop optical sensor for anions based on hydrogen bonding interaction.

ASSOCIATED CONTENT

Supporting Information

pK_a scheme, absorption and emission spectra at different pH, absorption and emission spectra in the absence and presence CN⁻, other binding curves, Job plots, method for detection limit, ¹H NMR, ¹H–¹H COSY, and HMBC spectra, Cartesian coordinates of the optimized structure. This material is available free of charge via the Internet at <http://pubs.acs.org>.

AUTHOR INFORMATION

Corresponding Author

*E-mail: cesybh@mail.sysu.edu.cn.

Notes

The authors declare no competing financial interest.

ACKNOWLEDGMENTS

This work was supported by the NSF of China (20771104 and 21071154), and Sun Yat-Sen University. We would also like to thank Professor Tong-Bu Lu and Dr. Long Jiang for providing help.

REFERENCES

- (1) Sessler, J. L.; Gale, P. A.; Cho, W.-S., *Anion Receptor Chemistry*; The Royal Society of Chemistry: Cambridge, U.K., 2006.
- (2) Amendola, V.; Fabbri, L. *Chem. Commun.* **2009**, 513–531.
- (3) Kim, S. K.; Sessler, J. L. *Chem. Soc. Rev.* **2010**, 39, 3784–3809.
- (4) Li, A.-F.; Wang, J.-H.; Wang, F.; Jiang, Y.-B. *Chem. Soc. Rev.* **2010**, 39, 3729–3745.
- (5) Duke, R. M.; Veale, E. B.; Pfeiffer, F. M.; Kruger, P. E.; Gunnlaugsson, T. *Chem. Soc. Rev.* **2010**, 39, 3936–3953.
- (6) Kang, S. O.; Llinares, J. M.; Day, V. W.; Bowman-James, K. *Chem. Soc. Rev.* **2010**, 39, 3980–4003.
- (7) Gale, P. A. *Acc. Chem. Res.* **2011**, 44, 216–226.
- (8) Dydio, P.; Lichosyt, D.; Jurczak, J. *Chem. Soc. Rev.* **2011**, 40, 2971–2985.
- (9) Vennesland, B.; Conn, E. E.; Knowles, C. J.; Westly, J.; Wissing, F., *Cyanide in Biology*; Academic Press: London, 1981.
- (10) Koenig, R. *Science* **2000**, 287, 1737–1738.
- (11) Kubik, S. *Chem. Soc. Rev.* **2010**, 39, 3648–3663.
- (12) Xu, Z.; Chen, X.; Kim, H. N.; Yoon, J. *Chem. Soc. Rev.* **2010**, 39, 127–137.
- (13) Cho, D.-G.; Sessler, J. L. *Chem. Soc. Rev.* **2009**, 38, 1647–1662.
- (14) Zelder, F. H.; Mannel-Croise, C. *Chimia* **2009**, 63, 58–62.
- (15) Badugu, R.; Lakowicz, J. R.; Geddes, C. D. *J. Am. Chem. Soc.* **2005**, 127, 3635–3641.
- (16) Palomares, E.; Martínez-Díaz, M. V.; Torres, T.; Coronado, E. *Adv. Funct. Mater.* **2006**, 16, 1166–1170.
- (17) Lee, K.-S.; Kim, H.-J.; Kim, G.-H.; Shin, I.; Hong, J.-I. *Org. Lett.* **2008**, 10, 49–51.
- (18) Kim, Y.; Zhao, H.; Gabbai, F. P. *Angew. Chem., Int. Ed.* **2009**, 48, 4957–4960.
- (19) Jo, J.; Lee, D. *J. Am. Chem. Soc.* **2009**, 131, 16283–16291.
- (20) Mannel-Croise, C.; Zelder, F. *Inorg. Chem.* **2009**, 48, 1272–1274.
- (21) Vallejos, S.; Estevez, P.; Garcia, F. C.; Serna, F.; de la Pena, J. L.; Garcia, J. M. *Chem. Commun.* **2010**, 46, 7951–7953.
- (22) Dai, Z.; Boon, E. M. *J. Am. Chem. Soc.* **2010**, 132, 11496–11503.
- (23) Tetilla, M. A.; Aragoni, M. C.; Arca, M.; Caltagirone, C.; Bazzicalupi, C.; Bencini, A.; Garau, A.; Isaia, F.; Laguna, A.; Lippolis, V.; Meli, V. *Chem. Commun.* **2011**, 47, 3805–3807.
- (24) Mashraqui, S. H.; Betkar, R.; Chandiramani, M.; Estarellas, C.; Frontera, A. *New J. Chem.* **2011**, 35, 57–60.
- (25) Yuan, L.; Lin, W.; Yang, Y.; Song, J.; Wang, J. *Org. Lett.* **2011**, 13, 3730–3733.
- (26) Isaad, J.; El Achari, A. *Tetrahedron* **2011**, 67, 4196–4201.
- (27) Isaad, J.; El Achari, A. *Tetrahedron* **2011**, 67, 4939–4947.
- (28) Isaad, J.; Salaun, F. *Sens. Actuators, B* **2011**, 157, 26–33.
- (29) Isaad, J.; Achari, A. E. *Anal. Chim. Acta* **2011**, 694, 120–127.
- (30) Wu, X.; Xu, B.; Tong, H.; Wang, L. *Macromolecules* **2011**, 44, 4241–4248.
- (31) Park, I. S.; Heo, E.-J.; Kim, J.-M. *Tetrahedron Lett.* **2011**, 52, 2454–2457.
- (32) Kim, H. J.; Ko, K. C.; Lee, J. H.; Lee, J. Y.; Kim, J. S. *Chem. Commun.* **2011**, 47, 2886–2888.
- (33) Liu, Z.; Wang, X.; Yang, Z.; He, W. *J. Org. Chem.* **2011**, 76, 10286–10290.
- (34) Lv, X.; Liu, J.; Liu, Y.; Zhao, Y.; Chen, M.; Wang, P.; Guo, W. *Sens. Actuators, B* **2011**, 158, 405–410.
- (35) Lv, X.; Liu, J.; Liu, Y.; Zhao, Y.; Sun, Y.-Q.; Wang, P.; Guo, W. *Chem. Commun.* **2011**, 47, 12843–12845.
- (36) Kumari, N.; Jha, S.; Bhattacharya, S. *J. Org. Chem.* **2011**, 76, 8215–8222.
- (37) Lin, Y.-S.; Zheng, J.-X.; Tsui, Y.-K.; Yen, Y.-P. *Spectrochim. Acta, Part A* **2011**, 79, 1552–1558.
- (38) Li, G.-Y.; Song, P.; He, G.-Z. *Chin. J. Chem. Phys.* **2011**, 24, 305–310.
- (39) Jamkratoke, M.; Tumcharern, G.; Tuntulani, T.; Tomapatnaget, B. *J. Fluoresc.* **2011**, 21, 1179–1187.
- (40) Kim, H. J.; Lee, H.; Lee, J. H.; Choi, D. H.; Jung, J. H.; Kim, J. S. *Chem. Commun.* **2011**, 47, 10918–10920.
- (41) Kim, Y.; Huh, H.-S.; Lee, M. H.; Lenov, I. L.; Zhao, H.; Gabbai, F. P. *Chem.—Eur. J.* **2011**, 17, 2057–2062.
- (42) Liu, J.; Liu, Y.; Liu, Q.; Li, C.; Sun, L.; Li, F. *J. Am. Chem. Soc.* **2011**, 133, 15276–15279.
- (43) Ganesh, V.; Calatayud Sanz, M. P.; Mareque-Rivas, J. C. *Chem. Commun.* **2007**, 5010–5012.
- (44) Lou, X.; Zhang, L.; Qin, J.; Li, Z. *Chem. Commun.* **2008**, 5848–5850.
- (45) Shang, L.; Zhang, L.; Dong, S. *Analyst* **2009**, 134, 107–113.
- (46) Chung, S.-Y.; Nam, S.-W.; Lim, J.; Park, S.; Yoon, J. *Chem. Commun.* **2009**, 2866–2868.

- (47) Chen, X.; Nam, S.-W.; Kim, G.-H.; Song, N.; Jeong, Y.; Shin, I.; Kim, S. K.; Kim, J.; Park, S.; Yoon, J. *Chem. Commun.* **2010**, 46, 8953–8955.
- (48) Jung, H. S.; Han, J. H.; Kim, Z. H.; Kang, C.; Kim, J. S. *Org. Lett.* **2011**, 13, 5056–5059.
- (49) Wang, J.; Ha, C.-S. *Analyst* **2011**, 136, 1627–1631.
- (50) Hajizadeh, S.; Farhadi, K.; Forough, M.; Sabzi, R. E. *Anal. Methods* **2011**, 3, 2599–2603.
- (51) Helal, A.; Kim, S.; Kim, H. S. *Bull. Korean Chem. Soc.* **2011**, 32, 3123–3126.
- (52) Senapati, D.; Dasary, S. S. R.; Singh, A. K.; Senapati, T.; Yu, H. T.; Ray, P. C. *Chem.—Eur. J.* **2011**, 17, 8445–8451.
- (53) Lou, X.; Zhang, Y.; Qin, J.; Li, Z. *Chem.—Eur. J.* **2011**, 17, 9691–9696.
- (54) Yang, M.; He, J.; Hu, X.; Yan, C.; Cheng, Z.; Zhao, Y.; Zuo, G. *Sens. Actuators, B* **2011**, 155, 692–698.
- (55) Álvarez-Díaz, A.; Salinas-Castillo, A.; Camprubí-Robles, M.; Costa-Fernández, J. M.; Pereiro, R.; Mallavia, R.; Sanz-Medel, A. *Anal. Chem.* **2011**, 83, 2712–2718.
- (56) Liu, C.-Y.; Tseng, W.-L. *Chem. Commun.* **2011**, 47, 2550–2552.
- (57) Zhai, Y.; Jin, L.; Wang, P.; Dong, S. *Chem. Commun.* **2011**, 47, 8268–8270.
- (58) Maldonado, C. R.; Touceda-Varela, A.; Jones, A. C.; Mareque-Rivas, J. C. *Chem. Commun.* **2011**, 47, 11700–11702.
- (59) Zou, Q.; Li, X.; Zhang, J.; Zhou, J.; Sun, B.; Tian, H. *Chem. Commun.* **2012**, 48, 2095–2097.
- (60) Sun, S.-S.; Lees, A. J. *Chem. Commun.* **2000**, 1687–1688.
- (61) Sun, S.-S.; Lees, A. J.; Zavalij, P. Y. *Inorg. Chem.* **2003**, 42, 3445–3453.
- (62) Anzenbacher, P.; Tyson, D. S.; Jursikova, K.; Castellano, F. N. *J. Am. Chem. Soc.* **2002**, 124, 6232–6233.
- (63) Ros-Lis, J. V.; Martínez-Máñez, R.; Sancenón, F.; Soto, J.; Rurack, K.; Weisshoff, H. *Eur. J. Org. Chem.* **2007**, 2449–2458.
- (64) Gimeno, N.; Li, X.; Durrant, J. R.; Vilar, R. *Chem.—Eur. J.* **2008**, 14, 3006–3012.
- (65) Zimmermann-Dimer, L. M.; Reis, D. C.; Machado, C.; Machado, V. G. *Tetrahedron* **2009**, 65, 4239–4248.
- (66) Lin, Z.; Chen, H. C.; Sun, S.-S.; Hsu, C.-P.; Chow, T. J. *Tetrahedron* **2009**, 65, 5216–5221.
- (67) Lee, G. W.; Kim, N.-K.; Jeong, K.-S. *Org. Lett.* **2010**, 12, 2634–2637.
- (68) Saha, S.; Ghosh, A.; Mahato, P.; Mishra, S.; Mishra, S. K.; Suresh, E.; Das, S.; Das, A. *Org. Lett.* **2010**, 12, 3406–3409.
- (69) Kumar, V.; Rana, H.; Kaushik, M. P. *Analyst* **2011**, 136, 1873–1880.
- (70) Lee, D. Y.; Singh, N.; Satyender, A.; Jang, D. O. *Tetrahedron Lett.* **2011**, 52, 6919–6922.
- (71) Ramabhadran, R. O.; Hua, Y.; Li, Y.-j.; Flood, A. H.; Raghavachari, K. *Chem.—Eur. J.* **2011**, 17, 9123–9129.
- (72) Cametti, M.; Rissanen, K. *Chem. Commun.* **2009**, 2809–2829.
- (73) Hudnall, T. W.; Chiu, C.-W.; Gabbai, F. P. *Acc. Chem. Res.* **2009**, 42, 388–397.
- (74) Wade, C. R.; Broomsgrove, A. E. J.; Aldridge, S.; Gabbai, F. P. *Chem. Rev.* **2010**, 110, 3958–3984.
- (75) Amendola, V.; Bonizzoni, M.; Esteban-Gomez, D.; Fabbrizzi, L.; Licchelli, M.; Sancenón, F.; Taglietti, A. *Coord. Chem. Rev.* **2006**, 250, 1451–1470.
- (76) Mercer, D. J.; Loeb, S. J. *Chem. Soc. Rev.* **2010**, 39, 3612–3620.
- (77) Marcus, Y. J. *Chem. Soc., Faraday Trans.* **1991**, 87, 2995–2999.
- (78) Broomsgrove, A. E. J.; Addy, D. A.; Di Paolo, A.; Morgan, I. R.; Bresner, C.; Chislett, V.; Fallis, I. A.; Thompson, A. L.; Vidovic, D.; Aldridge, S. *Inorg. Chem.* **2010**, 49, 157–173.
- (79) Garcia-Espana, E.; Diaz, P.; Llinares, J. M.; Bianchi, A. *Coord. Chem. Rev.* **2006**, 250, 2952–2986.
- (80) Mullen, K. M.; Beer, P. D. *Chem. Soc. Rev.* **2009**, 38, 1701–1713.
- (81) Hua, Y. R.; Flood, A. H. *Chem. Soc. Rev.* **2010**, 39, 1262–1271.
- (82) Gong, H. Y.; Rambo, B. M.; Karnas, E.; Lynch, V. M.; Sessler, J. L. *Nat. Chem.* **2010**, 2, 406–409.
- (83) Custelcean, R.; Bock, A.; Moyer, B. A. *J. Am. Chem. Soc.* **2010**, 132, 7177–7185.
- (84) Jia, C.; Wu, B.; Li, S.; Huang, X.; Zhao, Q.; Li, Q.-S.; Yang, X.-J. *Angew. Chem., Int. Ed.* **2011**, 50, 486–490.
- (85) Li, S.; Jia, C.; Wu, B.; Luo, Q.; Huang, X.; Yang, Z.; Li, Q.-S.; Yang, X.-J. *Angew. Chem., Int. Ed.* **2011**, 50, 5721–5724.
- (86) Chudzinski, M. G.; McClary, C. A.; Taylor, M. S. *J. Am. Chem. Soc.* **2011**, 133, 10559–10567.
- (87) Anzenbacher, P.; Try, A. C.; Miyaji, H.; Jursikova, K.; Lynch, V. M.; Marquez, M.; Sessler, J. L. *J. Am. Chem. Soc.* **2000**, 122, 10268–10272.
- (88) Mizuno, T.; Wei, W.-H.; Eller, L. R.; Sessler, J. L. *J. Am. Chem. Soc.* **2002**, 124, 1134–1135.
- (89) Bond, A.; Haga, M. *Inorg. Chem.* **1986**, 25, 4507–4514.
- (90) Haga, M.; Ano, T.; Kano, K.; Yamabe, S. *Inorg. Chem.* **1991**, 30, 3843–3849.
- (91) Rillema, D.; Sahai, R.; Matthews, P.; Edwards, A.; Shaver, R.; Morgan, L. *Inorg. Chem.* **1990**, 29, 167–175.
- (92) Lin, Z.-H.; Ou, S.-J.; Duan, C.-Y.; Zhang, B.-G.; Bai, Z.-P. *Chem. Commun.* **2006**, 624–626.
- (93) Liu, F.; Wang, K.; Bai, G.; Zhang, Y.; Gao, L. *Inorg. Chem.* **2004**, 43, 1799–1806.
- (94) Han, M.-J.; Gao, L.-H.; Lu, Y.-Y.; Wang, K.-Z. *J. Phys. Chem. B* **2006**, 110, 2364–2371.
- (95) Fan, S.-H.; Zhang, A.-G.; Ju, C.-C.; Gao, L.-H.; Wang, K.-Z. *Inorg. Chem.* **2010**, 49, 3752–3763.
- (96) Quaranta, A.; Lachaud, F.; Herrero, C.; Guillot, R.; Charlot, M.-F.; Leibl, W.; Aukauloo, A. *Chem.—Eur. J.* **2007**, 13, 8201–8211.
- (97) Zapata, F.; Caballero, A.; Espinosa, A.; Tarraga, A.; Molina, P. *J. Org. Chem.* **2008**, 73, 4034–4044.
- (98) Kundu, T.; Mobin, S. M.; Lahiri, G. K. *Dalton Trans.* **2010**, 39, 4232–4242.
- (99) Saha, D.; Das, S.; Bhaumik, C.; Dutta, S.; Baitalik, S. *Inorg. Chem.* **2010**, 49, 2334–2348.
- (100) Bhaumik, C.; Das, S.; Saha, D.; Dutta, S.; Baitalik, S. *Inorg. Chem.* **2010**, 49, 5049–5062.
- (101) Das, S.; Saha, D.; Bhaumik, C.; Dutta, S.; Baitalik, S. *Dalton Trans.* **2010**, 39, 4162–4169.
- (102) Saha, D.; Das, S.; Maity, D.; Dutta, S.; Baitalik, S. *Inorg. Chem.* **2011**, 50, 46–61.
- (103) Bhaumik, C.; Saha, D.; Das, S.; Baitalik, S. *Inorg. Chem.* **2011**, 50, 12586–12600.
- (104) EPA National Primary Drinking Water Standards, 2003. <http://www.epa.gov/safewater/contaminants/index.html>.
- (105) Sprintschnik, G.; Sprintschnik, H.; Kirsch, P.; Whitten, D. J. *Am. Chem. Soc.* **1977**, 99, 4947–4954.
- (106) Xu, H.; Zheng, K.-C.; Deng, H.; Lin, L.-J.; Zhang, Q.-L.; Ji, L.-N. *New J. Chem.* **2003**, 27, 1255–1263.
- (107) Chao, H.; Ye, B. H.; Li, H.; Li, R. H.; Zhou, J. Y.; Ji, L. N. *Polyhedron* **2000**, 19, 1975–1983.
- (108) Wu, J.-Z.; Ye, B.-H.; Wang, L.; Ji, L.-N.; Zhou, J.-Y.; Li, R.-H.; Zhou, Z.-Y. *J. Chem. Soc., Dalton Trans.* **1997**, 1395–1402.
- (109) Chao, H.; Ye, B.-H.; Zhang, Q.-L.; Ji, L.-N. *Inorg. Chem. Commun.* **1999**, 2, 338–340.
- (110) Connors, K. *Binding Constants: The Measurement of Molecular Complex Stability*; Wiley: New York, 1987.
- (111) Van Houten, J.; Watts, R. J. *Am. Chem. Soc.* **1976**, 98, 4853–4858.
- (112) McClanahan, S. F.; Dallinger, R. F.; Holler, F. J.; Kincaid, J. R. *J. Am. Chem. Soc.* **1985**, 107, 4853–4860.
- (113) Frisch, M. J.; Trucks, G. W.; Schlegel, H. B.; Scuseria, G. E.; Robb, M. A.; Cheeseman, J. R.; Montgomery, J. A., Jr.; Vreven, T.; Kudin, K. N.; Barant, J. C.; Millam, J. M.; Iyengar, S. S.; Tomasi, J.; Barone, V.; Mennucci, B.; Cossi, M.; Scalmani, G.; Rega, N.; Petersson, G. A.; Nakatsuji, H.; Hada, M.; Ehara, M.; Toyota, K.; Fukuda, R.; Hasegawa, J.; Ishida, M.; Nakajima, T.; Honda, Y.; Kitao, O.; Nakai, H.; Klene, M.; Li, X.; Knox, J. E.; Hratchian, H. P.; Cross, J. B.; Bakken, V.; Adamo, C.; Jaramillo, J.; Gomperts, R.; Stratmann, R. E.; Yazyev, O.; Austin, A. J.; Cammi, R.; Pomelli, C.; Ochterski, J. W.;

Ayala, P. Y.; Morokuma, K.; Voth, G. A.; Salvador, P.; Dannenberg, J. J.; Zakrzewski, V. G.; Dapprich, S.; Daniels, A. D.; Strain, M. C.; Farkas, O.; Malick, D. K.; Rabuck, A. D.; Raghavachari, K.; Foresman, J. B.; Ortiz, J. V.; Cui, Q.; Baboul, A. G.; Clifford, S.; Cioslowski, J.; Stefanov, B. B.; Liu, G.; Liashenko, A.; Piskorz, P.; Komaromi, I.; Martin, R. L.; Fox, D. J.; Keith, T.; Al-Laham, M. A.; Peng, C. Y.; Nanayakkara, A.; Challacombe, M.; Gill, P. M. W.; Johnson, B.; Chen, W.; Wong, M. W.; Gonzalez, C.; Pople, J. *Gaussian 03, Revision D.01*; Gaussian Inc.: Wallingford, CT, 2005.

(114) Becke, A. D. *Phys. Rev. A: Gen. Phys.* **1988**, *38*, 3098–3100.

(115) Becke, A. D. *J. Chem. Phys.* **1993**, *98*, 5648–5652.

(116) Lee, C.; Yang, W.; Parr, R. G. *Phys. Rev. B: Condens. Matter Phys.* **1988**, *37*, 785–789.

(117) Hehre, W. J.; Radom, L.; Schleyer, P. v. R.; Pople, J. A. *Ab Initio Molecular Orbital Theory*; John Wiley & Sons: New York, 1986.

(118) Dolg, M.; Stoll, H.; Preuss, H. *Theor. Chim. Acta* **1993**, *85*, 441–450.

(119) Wedig, U.; Dolg, M.; Stoll, H. *Quantum Chemistry: The Challenge of Transition Metals and Coordination Chemistry*; Kluwer Academic Publishers: Dordrecht, The Netherlands, 1986.

(120) Steck, E. A.; Day, A. R. *J. Am. Chem. Soc.* **1943**, *65*, 452–456.

(121) Mo, H.-J.; Niu, Y.-L.; Zhang, M.; Qiao, Z.-P.; Ye, B.-H. *Dalton Trans.* **2011**, *40*, 8218–8225.

(122) Han, M.-J.; Gao, L.-H.; Wang, K.-Z. *New J. Chem.* **2006**, *30*, 208–214.

(123) Freys, J. C.; Bernardinelli, G.; Wenger, O. S. *Chem. Commun.* **2008**, 4267–4269.

(124) Liu, Y.; Han, B.-H.; Chen, Y.-T. *J. Phys. Chem. B* **2002**, *106*, 4678–4687.

(125) Roundhill, D. M. *Photochemistry and Photophysics of Metal Complexes*; Plenum Press: New York, 1994.

(126) Boiocchi, M.; Del Boca, L.; Esteban-Gómez, D.; Fabbrizzi, L.; Licchelli, M.; Monzani, E. *J. Am. Chem. Soc.* **2004**, *126*, 16507–16514.

(127) Balzani, V.; Sabbatini, N.; Scandola, F. *Chem. Rev.* **1986**, *86*, 319–337.

(128) Sessler, J. L.; Cai, J.; Gong, H.-Y.; Yang, X.; Arambula, J. F.; Hay, B. P. *J. Am. Chem. Soc.* **2010**, *132*, 14058–14060.

(129) Kuhn, N.; Eichele, K.; Steimann, M.; Al-Sheikh, A.; Doser, B.; Ochsenfeld, C. Z. *Anorg. Allg. Chem.* **2006**, *632*, 2268–2275.

(130) Metzger, A.; Lynch, V. M.; Anslyn, E. V. *Angew. Chem., Int. Ed. Engl.* **1997**, *36*, 862–865.

(131) Yoon, J.; Kim, S. K.; Singh, N. J.; Kim, K. S. *Chem. Soc. Rev.* **2006**, *35*, 355–360.

(132) Ion, L.; Morales, D.; Perez, J.; Riera, L.; Riera, V.; Kowenicki, R. A.; McPartlin, M. *Chem. Commun.* **2006**, 91–93.

(133) Steiner, T. *Angew. Chem., Int. Ed.* **2002**, *41*, 48–76.

(134) Koti, A. S. R.; Krishna, M. M. G.; Periasamy, N. *J. Phys. Chem. A* **2001**, *105*, 1767–1771.

(135) Ashokkumar, P.; Ramakrishnan, V. T.; Ramamurthy, P. *Chem.—Eur. J.* **2010**, *16*, 13271–13277.